ACTA CHEMICA SCANDINAVICA 26 (1972) 3662–3670

On the System Fe—Ni—Te

ERLING RØST and GUNVOR ÅKESSON

Kjemisk Institutt, Universitetet i Oslo, Oslo 3, Norway

The phase relations of the ternary system Fe–Ni–Te at 600°C have been examined mainly by X-ray diffraction and metallographic methods. A ternary equilibrium diagram of the system at 600°C is presented.

For the hexagonal NiAs–$Cd(OH)_2$ type phase which exists in both the binary systems Fe–Te and Ni–Te complete mutual interchange of iron and nickel is possible. For the two phases $FeTe_{0.9}$ and $Ni_{3+x}Te_2$, both having tetragonal structure of an intermediate type between the Fe_2As and PbO structure, only limited interchange of iron and nickel is possible. Between these phases a ternary phase with rhombohedral crystal structure exists. At 600°C this phase extends in the range 17–32 at. % Fe, 24–41 at. % Ni, and 41–45 at. % Te. At lower temperatures, however, the homogeneity region is more limited. For the phases $FeTe_2$ (marcasite structure) and $NiTe_{0.77}$ (orthorhombic structure) no extension in the ternary range could be observed.

Series of lattice constants *versus* composition are presented for some of the phases.

In the binary system *nickel-tellurium* a homogeneity region exists between the limits $NiTe_{0.67}$ and $NiTe_{0.7}$.[1,2] The structure is an intermediate between the Fe_2As and PbO type ($C38-B10$). Below 200–300°C the structure is monoclinic for nickel-rich, and orthorhombic for tellurium-rich samples. Above approximately 800°C the structure is of a face-centered cubic type. A phase with composition $NiTe_{0.77}$ has orthorhombic crystal structure.[2] The homogeneity region of this phase is rather narrow, whereas the phase region with hexagonal NiAs–$Cd(OH)_2$-type structure ($B8-C6$) extended from about $NiTe_{1.09}$ to $NiTe_2$.[2]

Also in the *iron-tellurium* system there exists a tetragonal phase with $C38-B10$ type structure.[3] The composition is given as $FeTe_{0.9}$. A phase with composition $FeTe_{1.1}$ is stable around 750°C.[3] According to Grønvold *et al.*[3] the NiAs–$Cd(OH)_2$ type phase region is stable above 488°C and is extended from $FeTe_{1.4}$ to $FeTe_{1.5}$. Chiba [4] suggests a broader homogeneity range at 600°C. The most tellurium-rich phase $FeTe_{1.95}-FeTe_{2.10}$ has mascasite structure type ($C18$).[3]

Iron and nickel form a continuous range of homogeneity with *fcc* structure above 911°C (γ-phase). Below this temperature iron has a *bcc* structure (α-phase), and only limited amounts of nickel can be dissolved in this phase. According to Owen and Liu [5] the α-phase can dissolve about 3.7 at. % Ni at 600°C, whereas the γ-phase exists from about 17.3 to 100 at. % Ni at that temperature. The ferromagnetic Curie temperature of the α-phase is about 780°C and the corresponding temperature for the most iron-rich samples of the γ-phase is near 400°C.

The metal-rich part of the *ternary system* Fe–Ni–Te has been examined by Stevels.[6] In the tetragonal phase $Fe_{1.12}Te$ about 40 at. % of the iron can be replaced by nickel in slowly cooled samples, and in the phase $Ni_{3\pm x}Te_2$ about 30 at. % of the nickel can be replaced by iron. The structure of the latter phase changes from tetragonal to orthorhombic below 200–300°C. In the ternary region a phase with composition $Fe_{1.5}Ni_{1.5}Te_2$ and rhombohedral structure was found.[6] A limited variation of the tellurium/metal ratio is possible. The lattice constants of this phase are given as $a = 7.213$ Å and $\alpha = 30°50'$. A crystal structure is suggested based on the space group $R\bar{3}m$.

EXPERIMENTAL

The *tellurium* used in this investigation was a 5N sample from Koch-Light Laboratories. *Nickel* was prepared from "NiO, low in Co and Fe" from the British Drug Houses by reduction with deoxidized and dried hydrogen gas. After the reduction the metal was annealed in hydrogen at 1000°C. The *iron*, "*Ferrum reductum pro analysi*" from E. Merck A. G., was annealed at 1000°C in hydrogen atmosphere.

The alloys were prepared by heating to fusion calculated amounts of the elements in evacuated and sealed silica tubes. Some samples were re-annealed for a week after being finely ground in a mortar. The most tellurium-rich samples were made by adding calculated amounts of tellurium to samples richer in metal. The mixture had to be annealed for some days in order to obtain equilibrium conditions.

The alloys were examined mainly by metallographic and X-ray methods. X-Ray powder patterns were obtained in a Guinier-type focusing camera, using monocromatic $CuK\alpha_1$ radiation. Silicon ($a = 5.43054$ Å) [7] was used as calibration standard. High temperature X-ray investigations were carried out in a 19 cm Unicam Camera with the samples sealed in thin-walled silica capillaries. Density measurements were carried out at 25°C by a vacuum pycnometric method. The presence of metal phases was detected by means of a permanent magnet. Further magnetic properties were measured by the Faraday method.

Table 1. Phases present at 600°C in the system Fe–Ni–Te. The composition range in at. % of each element is given.

Phase	Composition range Fe	Ni	Te	Structure type
A	32.3 – 33.9	0	66.1 – 67.7	*C*18, Marcasite
B	0 – 41.7	0 – 46.8	53.2 – 66.7	*B*8 – *C*6, NiAs – $Cd(OH)_2$
C	36 – 53	0 – 19	46 – 47	*C*38 – *B*10, Fe_2As – PbO
D	17 – 32	24 – 41	41 – 45	Rhombohedral
E	0	56.4	43.6	Orthorhombic
F	0 – 13	45 – 60	40 – 42	*C*38 – *B*10 type
α-Me	96.3 – 100	0 – 3.7	0	Body centered cubic
γ-Me	0 – 82.7	17.3 – 100	0	Face centered cubic

Table 2. Compositions of the samples in at. % and phases present at 600°C.

No.	Fe	Ni	Te	Phases	No.	Fe	Ni	Te	Phases	No.	Fe	Ni	Te	Phases
1	32.0	1.3	66.7	A+B	30	36.0	16.0	48.0	B+C	59	36.0	22.0	42.0	C+D+γ-Me
2	22.2	11.1	66.7	A+B+Te	31	28.0	24.0	48.0	B+C+D	60	33.0	25.0	42.0	D+γ-Me
3	20.3	13.0	66.7	A+B+Te	32	52.0	1.0	47.0	C	61	29.0	29.0	42.0	D+γ-Me
4	16.7	16.7	66.7	B+Te	33	48.0	6.0	46.0	C+γ-Me	62	20.0	38.0	42.0	D
5	10.3	23.0	66.7	B+Te	34	44.0	10.0	46.0	C	63	18.0	40.0	42.0	D
6	1.3	32.0	66.7	B	35	41.0	13.0	46.0	B+C	64	15.0	43.0	42.0	D+F
7	17.0	17.0	66.0	B	36	36.0	18.0	46.0	B+C	65	14.0	44.0	42.0	D+F
8	29.8	6.0	64.2	A+B	37	38.0	17.0	45.0	C+γ-Me	66	12.0	46.0	42.0	F
9	17.9	17.9	64.2	B	38	35.0	20.0	45.0	C+D	67	8.0	50.0	42.0	B+F
10	36.0	0.0	64.0	A+B	39	33.0	22.0	45.0	C+D	68	2.0	56.0	42.0	B+F
11	29.2	6.8	64.0	B	40	31.5	23.5	45.0	C+D	69	20.0	39.0	41.0	D+γ-Me
12	37.0	0.0	63.0	B	41	30.0	25.0	45.0	D	70	17.1	41.9	41.0	D+γ-Me
13	36.9	1.2	61.9	B	42	27.5	27.5	45.0	B+D	71	15.0	44.0	41.0	D+F+γ-Me
14	19.3	19.3	61.4	B	43	25.0	30.0	45.0	B+D	72	13.5	45.5	41.0	F+γ-Me
15	41.0	0.0	59.0	B	44	13.3	41.8	44.9	B+D+F	73	6.0	53.5	40.5	F+γ-Me
16	36.9	4.3	58.8	B	45	50.0	6.0	44.0	C+α-Me	74	56.0	4.0	40.0	C+α-Me
17	42.0	0.0	58.0	B+C	46	48.0	8.0	44.0	C+γ-Me	75	43.0	7.0	40.0	C+γ-Me
18	35.0	7.0	58.0	B+C	47	38.0	18.0	44.0	C+γ-Me	76	41.0	19.0	40.0	C+D+γ-Me
19	26.0	16.0	58.0	B+C	48	36.0	20.0	44.0	C+D+γ-Me	77	36.0	24.0	40.0	D+γ-Me
20	19.4	22.6	58.0	B	49	33.0	23.0	44.0	C+D	78	30.0	30.0	40.0	D+γ-Me
21	31.0	12.0	57.0	B+C	50	32.0	24.0	44.0	D	79	19.0	41.0	40.0	D+γ-Me
22	21.8	21.8	56.4	B+C	51	28.0	28.0	44.0	D	80	15.0	45.0	40.0	F+γ-Me
23	14.0	30.0	56.0	B	52	21.0	35.0	44.0	B+D	81	48.0	22.0	30.0	C+D+γ-Me
24	9.4	36.6	54.0	B+D	53	13.0	43.0	44.0	B+D+F	82	46.0	24.0	30.0	D+γ-Me
25	19.0	28.5	52.5	B+C+D	54	1.0	55.0	44.0	B+F	83	52.6	19.6	27.8	C+D+γ-Me
26	24.0	24.0	52.0	B+C	55	0.6	55.4	44.0	B+E+F	84	30.0	45.0	25.0	D+γ-Me
27	5.0	43.5	51.5	B+D+F	56	26.0	31.0	43.0	D	85	29.0	46.0	25.0	D+F+γ-Me
28	0.5	48.5	51.0	B+F	57	19.0	38.1	42.9	B+D	86	27.0	48.0	25.0	F+γ-Me
29	49.7	2.4	47.9	B+C	58	0.5	56.8	42.7	B+E+F					

PHASE RELATIONS AT 600°C

In the present paper the homogeneity ranges are denoted with capital letters, and the extensions of them are given in Table 1. The gross composition of the different samples and the phases present at 600°C are listed in Table 2. The samples are numbered in order of increasing metal content. In Fig. 1 the compositions are plotted in a ternary at. % plot. The phase limits are indicated, and also the directions of some of the tie lines.

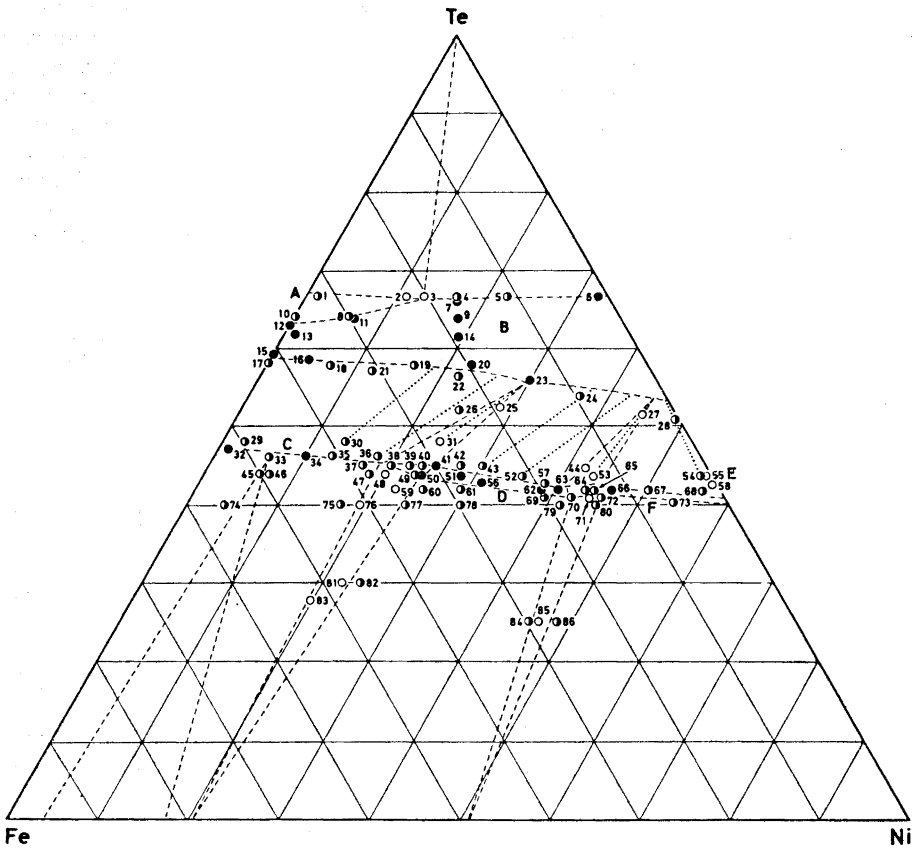

Fig. 1. At. % plot of alloy compositions. Filled, half filled, and open circles represent one, two, or three phases, respectively, at 600°C. Broken lines show boundaries between the different phase regions, and dotted lines show tie line directions determined. The single phase regions are denoted by capital letters.

In the *phase A* ($FeTe_2$) with marcasite type structure no substitution of nickel for iron was observed in quenched samples. Thus, X-ray photographs of sample 1 containing only 1.3 at. % nickel clearly showed the reflections

from phase B in addition to those from the marcasite type phase. It should be pointed out that in the corresponding selenide, $FeSe_2$, about 19 at. % of the Fe atoms can be replaced by Ni at 580°C.[8]

Neither could any mutual interchange of iron and nickel be observed in the *phase E* ($NiTe_{0.77}$). For the rest of the phases, however, extended homogeneity ranges exist in the ternary region at 600°C.

Phase B, NiAs–Cd(OH)$_2$-type. Reexamination of the phase limits in the binary iron–tellurium system shows an extension from approximately $FeTe_{1.4}$ to about $FeTe_{1.7}$ at 600°C. At lower temperatures the phase region is obviously less extended. In agreement with Grønvold *et al.*[3] the structure of $FeTe_{1.4}$ was found to be monoclinic, whereas the structure of samples rich in tellurium is hexagonal. In this phase iron can be successively replaced by nickel, and as the Ni/Fe ratio increases the maximum tellurium content in the phase increases. A break in the phase limit is observed at a Ni/Fe ratio of about 0.67. At the metal-rich limit of the phase the metal content increases with increase of the Ni/Fe ratio. In Table 3 the lattice constants along the tellurium-rich and also along the metal-rich boundaries of phase B are given. Along both boundaries the c/a ratio decreases considerably as nickel is substituted for iron.

Table 3. Lattice constants (Å) and unit cell volume of phase B measured along tellurium-rich and metal-rich boundaries. The samples were quenched from 600°C. Hexagonal structure of $B8-C6$ type.

Sample No.	Composition	a	b	V	c/a
2	$Fe_{.222}Ni_{.111}Te_{.667}$	3.7940	5.569	69.43	1.468
3	$Fe_{.203}Ni_{.130}Te_{.667}$	3.7928	5.565	69.32	1.467
4	$Fe_{.167}Ni_{.167}Te_{.667}$	3.8130	5.491	69.14	1.440
5	$Fe_{.103}Ni_{.230}Te_{.667}$	3.8364	5.402	68.85	1.410
6	$Fe_{.013}Ni_{.321}Te_{.667}$	3.8549	5.273	67.86	1.369
[a]	$Ni_{.333}Te_{.667}$	3.8547	5.261	67.70	1.365
16	$Fe_{.369}Ni_{.043}Te_{.588}$	3.860	5.588	72.09	1.448
18	$Fe_{.350}Ni_{.070}Te_{.580}$	3.881	5.548	72.37	1.430
21	$Fe_{.310}Ni_{.120}Te_{.570}$	3.883	5.496	71.78	1.415
19	$Fe_{.260}Ni_{.160}Te_{.580}$	3.899	5.471	72.02	1.403
20	$Fe_{.194}Ni_{.226}Te_{.580}$	3.904	5.440	71.80	1.393
23	$Fe_{.140}Ni_{.300}Te_{.560}$	3.914	5.426	72.02	1.386
24	$Fe_{.094}Ni_{.366}Te_{.540}$	3.933	5.401	72.36	1.373
[a]	$Ni_{.478}Te_{.522}$	3.969	5.362	73.14	1.351

[a] According to Barstad *et al.*[2]

Phases in the metal-rich region. The phases C and F have similar crystal structures, but no continuous phase region seems to exist between them, at least not above room temperature. At 600°C the phase C can contain up to about 19 at. % nickel, and the phase F up to 13 at. % iron. When samples were slowly cooled to room temperature during one week, however, the gap between the phases C and F was considerably reduced. Lattice constants of

Table 4. Lattice constants (Å) and unit cell volume of phase C measured on samples quenched from 600°C. Tetragonal structure of $C38-B10$ type.

Sample No.	Composition	a	c	V	c/a
[a]	$Fe_{.526}Te_{.474}$	3.819	6.280	81.59	1.644
32	$Fe_{.52}Ni_{.01}Te_{.47}$	3.827	6.268	91.80	1.637
34	$Fe_{.44}Ni_{.10}Te_{.46}$	3.824	6.233	91.14	1.630
35	$Fe_{.41}Ni_{.13}Te_{.46}$	3.825	6.206	90.80	1.622
37	$Fe_{.38}Ni_{.17}Te_{.45}$	3.816	6.197	90.25	1.624
36	$Fe_{.36}Ni_{.18}Te_{.46}$	3.816	6.195	90.23	1.623
38	$Fe_{.35}Ni_{.20}Te_{.45}$	3.814	6.184	89.97	1.621

[a] According to Grønvold *et al.*[3]

samples from phase C are presented in Table 4. A decrease of both the a- and c-axis takes place when nickel is substituted for iron. At the same time a successive increase of the metal/tellurium ratio is observed in this phase.

The structure of most of the samples from the phase region F changes from tetragonal to orthorhombic symmetry during the quenching. The tetragonal structure was retained for only one sample, No. 66 ($Fe_{.12}Ni_{.46}Te_{.42}$). The lattice constants of this sample are $a = 3.791$ Å and $c = 6.104$ Å which corresponds to a unit cell volume of 87.74 Å^3. These lattice constants fit in well with what one would expect from phase C if a more extended replacement of Fe by Ni had been possible in this phase. Despite the fact that phases C and F have the same structure type no continuous homogeneity range exists between them. The lattice constants determined for the samples from phase F with orthorhombic structure are in good agreement with those reported by Stevels,[6] and are not presented here.

Between the phases C and F there exists a ternary phase with rhombohedral crystal structure (phase D). The extension of this phase is narrow when the samples are slowly cooled. Phase D was retained as a single phase only in sample No. 56 ($Fe_{.26}Ni_{.31}Te_{.43}$). As the temperature is raised the homogeneity region of the rhombohedral phase increases considerably. An extensive mutual interchangeability of iron and nickel is possible, whereas the variation in the metal/tellurium ratio is more limited. At 600°C the Fe/Ni ratio can vary from about 1.4 to 0.4. The quenched samples from both the iron-rich and nickel-rich part of phase D gave very diffuse X-ray powder patterns, possibly due to phase changes during the quenching. Therefore, the boundaries in this region were determined to a great extent by high temperature X-ray methods, and by microscopic examination of polished surfaces.

Lattice constants of some samples from the phase D region, with rhombohedral structure, are given in Table 5. The density at 25°C of sample 51 ($Fe_{.28}Ni_{.28}Te_{.44}$) was determined to be 7.18 g cm^{-3}. This corresponds to 5.94 tellurium atoms and 7.58 metal atoms per unit cell. It seems reasonable to believe that the unit cell contains exactly six tellurium atoms whereas the number of metal atoms can vary within certain limits due to varying occupation of partly occupied metal sites in the structure. This is also in accordance

Table 5. Lattice constants (Å) of phase D measured on samples quenched from 600°C.

Sample No.	Composition	Hexagonal		Rhombohedral	
		a	*c*	*a*	α(°)
43	$Fe_{.25}Ni_{.30}Te_{.45}$	3.969	20.37	7.166	32.16
49	$Fe_{.33}Ni_{.23}Te_{.44}$	3.976	20.39	7.174	32.18
50	$Fe_{.32}Ni_{.24}Te_{.44}$	3.975	20.37	7.167	32.20
51	$Fe_{.28}Ni_{.28}Te_{.44}$	3.972	20.34	7.157	32.22
52	$Fe_{.21}Ni_{.35}Te_{.44}$	3.970	20.44	7.189	32.06
56	$Fe_{.26}Ni_{.31}Te_{.43}$	3.976	20.52	7.214	32.00
57	$Fe_{.19}Ni_{.36}Te_{.43}$	3.956	20.52	7.213	31.84
61	$Fe_{.29}Ni_{.29}Te_{.42}$	3.978	20.54	7.152	31.96

with the observed increase of lattice dimensions with increase of the metal/tellurium ratio. (The crystal structure of the rhombohedral phase has been examined on basis of single crystals, and results will be published separately.)

Two and three phase regions. In two phase fields the phases existing in equilibrium with each other at a certain temperature are connected through a so-called tie line. Three phase fields are limited by three tie lines which show the compositions of the three phases existing in equilibrium with each other. The positions of three phase fields were determined by phase analyses carried out by X-ray and metallographic methods. Some tie line directions in the region between phase B and the phases richer in metal were determined by lattice constant comparisons. Lattice constants of phase B in some two and three phase samples were determined, and the composition of this phase was then estimated by comparison with the lattice constants determined for the metalrich boundary of phase B (*cf.* Table 3). The results are given in Table 6.

Table 6. Compositions of phase B in two and three phase samples. The estimations are based on lattice constants comparisons.

Sample No.	Gross composition	Phases present	Lattice constants (Å)		Estimated composition of phase B
			a	*c*	
30	$Fe_{.36}Ni_{.16}Te_{.48}$	B+C	3.905	5.450	$Fe_{.23}Ni_{.19}Te_{.58}$
36	$Fe_{.36}Ni_{.16}Te_{.48}$	B+C	3.913	5.438	$Fe_{.18}Ni_{.26}Te_{.56}$
31	$Fe_{.28}Ni_{.24}Te_{.48}$	B+C+D	3.915	5.418	$Fe_{.14}Ni_{.03}Te_{.56}$
43	$Fe_{.30}Ni_{.25}Te_{.45}$	B+D	3.938	5.403	$Fe_{.09}Ni_{.37}Te_{.54}$
52	$Fe_{.21}Ni_{.35}Te_{.44}$	B+D	3.952	5.384	$Fe_{.04}Ni_{.42}Te_{.54}$
53	$Fe_{.13}Ni_{.43}Te_{.44}$	B+D+F	3.959	5.374	$Fe_{.03}Ni_{.44}Te_{.53}$
54	$Fe_{0.1}Ni_{.55}Te_{.44}$	B+F	3.972	5.366	$Fe_{.01}Ni_{.47}Te_{.52}$

In order to determine the boundaries of the three phase region containing phase C in equilibrium with the two metal phases α-Me and γ-Me, a magnetic examination was found to be suitable. High temperature magnetic measurements showed that sample 45 ($Fe_{.50}Ni_{.06}Te_{.44}$) has a strong, field strength

dependent magnetic susceptibility up to about 780°C. This corresponds to the Curie point of the *bcc* α-phase. Sample 46 ($Fe_{.48}Ni_{.08}Te_{.44}$), however, lost its ferromagnetism below 500°C. This strongly indicates that the metal phase in the latter sample is of the *fcc* type whereas sample 45 contains the *bcc*-type metal.

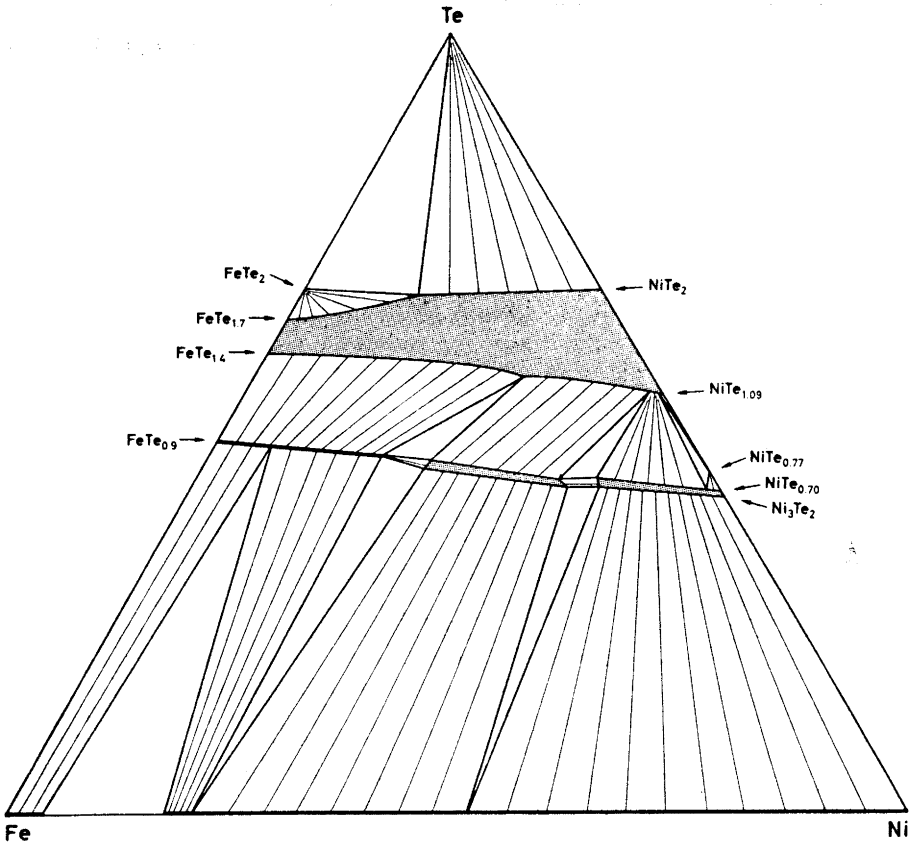

Fig. 2. Ternary phase diagram at 600°C of the system Fe–Ni–Te. Single phase regions are shown as dotted areas or heavy lines, two phase fields are indicated with some tie lines, and three phase fields are shown as open triangles.

The equilibrium diagram at 600°C of the condensed Fe–Ni–Te system is presented in Fig. 2. The extensions of the single phase fields and the two and three phase areas are shown. Tie line directions in the two phase fields are indicated.

REFERENCES

1. Kok, R. B., Wiegers, G. A. and Jellinek, F. *Rec. Trav. Chim.* **84** (1965) 1585.
2. Barstad, J., Grønvold, F., Røst, E. and Vestersjø, E. *Acta Chem. Scand.* **20** (1966) 2856.
3. Grønvold, F., Haraldsen, H. and Vihovde, J. *Acta Chem. Scand.* **8** (1954) 1927.
4. Chiba, S. *J. Phys. Soc. Japan* **10** (1955) 837.
5. Owen, E. A. and Liu, Y. H. *J. Iron Steel Inst. (London)* **163** (1949) 132.
6. Stevels, A. L. N., *Thesis, Philips Res. Reports, Suppl. No. 9* (1969).
7. Parrish, W. *Acta Cryst.* **13** (1960) 838.
8. Røst, E. and Haugsten, K. *Acta Chem. Scand.* **23** (1969) 388.

Received April 21, 1972.